ACS APPLIED MATERIALS & INTERFACES

Research Article

www.acsami.org

Bromination of Graphene: A New Route to Making High Performance Transparent Conducting Electrodes with Low Optical Losses

Ahmed E. Mansour, Sukumar Dey, and Aram Amassian*

Division of Physical Sciences and Engineering, Solar and Photovoltaics Engineering Research Center (SPERC), King Abdullah University of Science and Technology (KAUST), Thuwal 23955-6900, Saudi Arabia

Minas H. Tanielian

Boeing Research and Technology, Seattle, Washington 98124-2499, United States

Supporting Information

ABSTRACT: The unique optical and electrical properties of graphene have triggered great interest in its application as a transparent conducting electrode material and significant effort has been invested in achieving high conductivity while maintaining high transparency. Doping of graphene has been a popular route for reducing its sheet resistance, but this has typically come at a significant loss in optical transmittance. We demonstrate doping of few layers graphene (FLG) with bromine as a means of enhancing the conductivity via intercalation without major optical losses. Our results demonstrate the encapsulation of bromine within the FLG, leading to air-stable transparent conducting electrodes with 5-fold improvement of sheet resistance reaching ~180 Ω/□ at the cost of only 2−3% loss of optical transmittance. The remarkably low trade-off in optical transparency leads to the highest enhancements in the figure of merit reported thus far for FLG. Furthermore, we tune the work function by up to 0.3 eV by tuning the bromine content. These results should help pave the way for further development of graphene as a potential substitute to transparent conducting polymers and metal oxides used in optoelectronics, photovoltaics, and beyond.

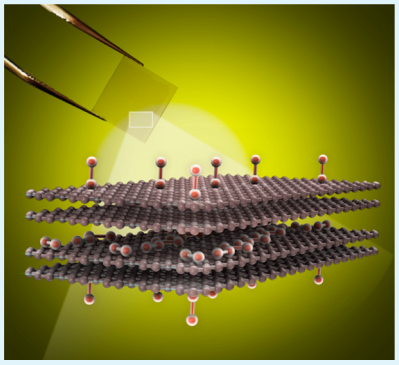

KEYWORDS: *graphene, few layers graphene, transparent conducting electrodes, doping, bromine*

INTRODUCTION

Since its discovery in 2004,[1] the unique properties of graphene have sparked tremendous interest and interdisciplinary research aimed toward integrating it into a wide range of emerging applications.[2] Mechanically, it is the strongest known material with Young's modulus of 1 TPa and intrinsic strength of 130 GPa.[3] Moreover, graphene exhibits high thermal stability and a superior conductivity of 5300 W m^{-1} K^{-1},[4,5] whereas charge transport in graphene is ballistic on the submicron scale with a fundamental limit of carrier mobility of 200 000 $cm^2V^{-1}s^{-1}$ and a carrier density on the order of 10^{12} cm^{-2}.[6] Optically, graphene is also intriguingly transparent, as a single layer absorbs 2.3% of white light with reflectance of less than 0.1% at all wavelengths.[7]

The high optical transmittance, electrical conductivity, flexibility and chemical stability of graphene have triggered great interest in its application as a transparent conducting electrode (TCE) material in optoelectronic devices and as a potential replacement for tin-doped indium oxide (ITO).[8−11] ITO is currently the most used TCE material, however, because of the relative scarcity of indium in the face of growing demand,[12] chemical stability issues[13] and its rigidity,[8] a replacement material that can meet the performance of ITO, and be mechanically flexible and chemically stable has been the subject of much research.[14−16] Large scale production methods for graphene such as chemical vapor deposition (CVD) on metals typically yield polycrystalline samples that are considerably more defective and impure after transfer, resulting in inferior conductivity as compared with theoretical predictions and measurements on mechanically exfoliated graphene.[17] Doping of graphene with foreign atoms and molecules has been a popular and successful route to significantly reducing its sheet resistance, with the bonus of also controlling the work function of the modified graphene.[9,18,19] However, the improvements of conductivity almost always come at a heavy cost of loss of optical transmittance.[9,20,21] For instance, doping a single layer graphene (SLG) sheet with metal chlorides results in a decrease of transmittance of 3.4% for $AuCl_3$ and 16.2% for $PdCl_3$ while only reducing the sheet resistance by half. At best, this leads to a slight improvement of the figure of merit (FoM) for transparent conducting graphene electrodes, defined as the ratio of the DC conductivity to the optical conductivity of the sample, but mostly results in a decrease of FoM.[22]

Received: April 16, 2015
Accepted: July 22, 2015
Published: July 22, 2015

DOI: 10.1021/acsami.5b03274
ACS Appl. Mater. Interfaces 2015, 7, 17692−17699

Bromine doping of carbon based materials was reported decades ago, and has been demonstrated to increase the electrical conductivity of optically thick graphite,[23,24] carbon nanotubes,[25,26] and polyacetelene.[27] Supermetallic conductivity of bromine-intercalated graphite has even been achieved via bromine vapor exposure of highly ordered pyrolytic graphite (HOPG).[28] The increase in conductivity was attributed to a parallel integration of weakly coupled p-doped graphene sheets. Bromine intercalated graphite compounds (Br-GIC) exist as a stage 2 intercalation compound, meaning that intercalation occurs at every second layer.[29,30] The p-doping nature of bromine into graphene has been confirmed by density functional theory (DFT) studies, suggesting a charge transfer toward physically adsorbed bromine species on graphene without disrupting its basal plane.[31] Physically adsorbed bromine on graphene has been previously achieved via vapor exposure and intercalation has been observed for films more than 2 layers in thickness. Both mechanisms of surface adsorption and intercalation were found not to disrupt the basal plane of graphene and led to high p-type doping density.[30] Enhancement of the conductivity and up-shifting of the work function for thinner but still optically opaque multilayered graphene (30−60 layers) and thick graphite (10 μm) by bromine vapor exposure was also recently reported, implying a strong thickness dependence of conductivity enhancement as the thick graphite samples exhibited larger improvement than multilayer graphene.[32] Covalently bonded bromine on graphene has also been reported by a microwave spark assisted method, but this reduces the conductivity of pristine graphene.[33] Given the well-known reactivity and volatility of bromine, it is not surprising to find that bromination of SLG, layer-by-layer stacked graphene (LLG) and few layers graphene (FLG) has not been investigated experimentally, nor has the transparency of these layers been evaluated and compared with other graphene TCE doping schemes. Nevertheless, bromine is well-known to readily intercalate into graphite at room temperature due to the high vapor pressure of bromine, making it possible to minimize covalent bonding promoted at elevated temperature.[34] We therefore take the view that bromine may indeed intercalate into FLG films and be sufficiently stabilized by virtue of self-encapsulation in between graphene sheets to explore the electrical and optical benefits of bromine-intercalated FLG in the context of TCE applications.

Herein, we report the successful bromine doping of graphene in inert atmosphere resulting in air-stable transparent conducting electrodes with up to 5-fold increase of conductivity at the cost of only 2−3% loss of optical transmittance in the case of FLG and 0.8% in case of SLG. The remarkably low trade-off in optical transparency for the conductivity boost leads to the highest enhancements in FoM for any doping scheme reported thus far. The FLG (4 to 10 layers) samples show the best results in terms of FoM enhancement as well as doping stability, mainly due to the encapsulation of bromine by the intercalation process in between the graphene sheets, as demonstrated by scanning tunneling microscopy (STM) analysis. Moderate temperature and exposure conditions ensure bromine is mostly physically adsorbed, leading to charge transfer doping of graphene, rather than covalent bonding which disrupts the basal plane of the graphene sheets and reduces their conductivity.[33,35] These developments, at the crossroads of bulk graphite and graphene, should help pave the way for further development in the area of graphene-based highly transparent conducting electrodes for a wide range of optoelectronic and photovoltaic applications.

RESULTS AND DISCUSSION

FLG samples prepared by CVD on Ni were lifted off and transferred onto glass substrates according to previously established recipes,[36] and subsequently exposed to bromine vapor at room temperature in inert atmosphere of two different contamination levels, namely, a glovebox (Gbox) with <0.1 ppm of O_2 and H_2O and a nitrogen filled glovebag (Gbag) with 2000 ppm of O_2 and 2500 ppm of H_2O. Importantly, all samples were washed in ethanol to remove excess and possibly weakly adsorbed bromine from the surface and grain boundaries prior to further handling and analysis, a condition we found to be very important for subsequent air stability of intercalated samples. Raman spectroscopy reveals no changes in the FLG structure after transfer from Ni to glass (Figure 1a),

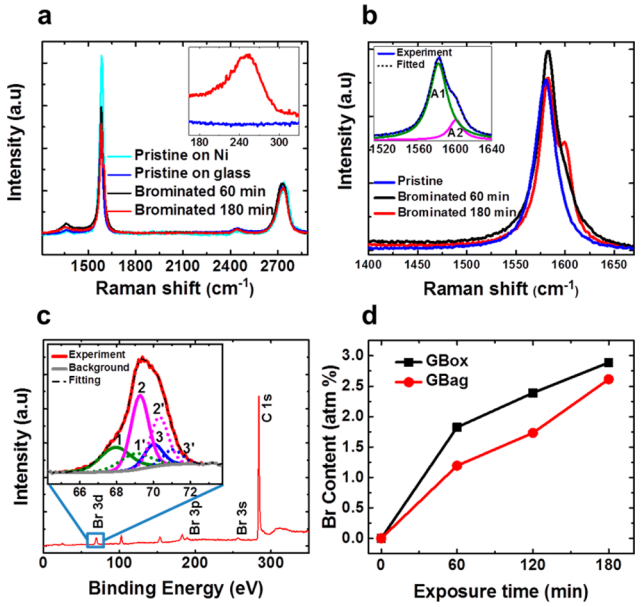

Figure 1. (a) Raman spectra taken of pristine FLG before and after transfer from a Ni film to a glass substrate and subsequently brominated (Gbag) for 60 and 180 min. The inset in panel a focuses on the region around the Br−Br stretching mode at 250 cm^{-1}. (b) G-peak variation upon bromination and splitting into doublet peaks (inset). (c) XPS survey scan of a brominated FLG sample (Gbox) for 180 min. The inset shows a high-resolution scan of the Br 3d peak. (d) Evolution of bromine content (at %) with increasing exposure time for bromination experiments performed inside the glovebox (black) and the glovebag placed in a fume hood (red). The Br 3d peak shifts to lower binding energy when using HBr as dopant, instead of Br_2, indicating that HBr is not a strong presence in the Br_2 intercalation experiments in inert atmosphere (Supporting Information).

where pristine FLG samples showed the typical Raman spectrum of CVD grown graphene on nickel, with a G-peak at 1580 cm^{-1} and a 2D-peak at 2725 cm^{-1}. A very small D-peak is observed at 1350 cm^{-1}, indicating the presence of defects and grain boundaries in the graphene plane. These are believed to result from the patchy nature of the film and wrinkles present due to the difference of the thermal coefficient of expansion between graphene and the Ni film.[37,38] Upon exposure to bromine, we observe a broadening of the G-peak, which continues to broaden with increased exposure time, to a point

DOI: 10.1021/acsami.5b03274
ACS Appl. Mater. Interfaces 2015, 7, 17692−17699

where it splits after 180 min of exposure as shown in the close up view in Figure 1b. The G-peak splitting into doublet peaks has been clearly observed in Br-GIC and was reported to consist of a graphitic band at 1580 cm^{-1} resulting from graphite surrounded region (A_1), and a stiffened band at 1600 cm^{-1} from graphitic planes adjacent to bromine (A_2).[35] Even though these two bands are not as clearly formed in FLG samples as in Br-GIC, we surmise that the fitted peaks in the G-peak of our samples, having the same separation, result from a similar mechanism, strongly pointing to intercalation. The characteristic G-peak was fitted using two Gaussian peaks A_1 and A_2, separated approximately by 20 cm^{-1} for all brominated samples (inset of Figure 1b). The increase of the intensity ratio A_2/A_1 with exposure time, even after ethanol wash, indicates increased bromine uptake by the sample with increasing exposure time (as shown in Figure S2). The intensity ratio of A_2/A_1 peaks is sensitive to the relative number of the graphene-bound layers and Br-bound layers, as well as to the molecular alignment of bromine between the sheets of graphene. A higher degree of molecular alignment of Br is expected to promote the growth of the A_2 peak.[35] Since the FLG films are of a patchy nature and vary laterally in the number of layers from 4 to 10 and exhibit different in-plane orientations, they lead to nonuniform intercalated layer formations in terms of the number and orientation of molecules. The higher density of grain boundaries and edges in FLG films is expected to promote incorporation of bromine at these sites without any specific molecular orientation. All of these factors should diminish the A_2 peak intensity as compared to the A_1 peak and result in a less pronounced peak splitting in Br-FLG than in Br-GIC, where HOPG has uniformly extended sheets of graphene throughout the sample. These features may promote higher bromine density at these specific sites, while the graphitic band at 1580 cm^{-1} continues to dominate the spectrum. The graphitic component of the G-peak (A_1) is blue-shifted in brominated graphene which is in line with previous Raman studies on doped graphene.[39] A Br−Br stretching mode peak appears in the spectrum at around 250 cm^{-1} (inset of Figure 1a) and is downshifted compared to that of free bromine molecules (323 cm^{-1}) and solid bromine (300 cm^{-1}).[35] This peak was previously reported around 240 cm^{-1} for both Br-GIC compounds and bromine doped mechanically exfoliated multilayer graphene.[30,40] At this position, the bromine peak can be related to either bromine molecules or to an anionic bromine mode. The blue shift of the G-peak and the red shift in the Br_2 stretching mode at 250 cm^{-1} both point to charge transfer occurring between Br_2 molecules and graphene.

The doping of FLG with bromine is further confirmed by X-ray photoelectron spectroscopy (XPS) performed on samples exposed to bromine in both Gbox and Gbag environments. In Figure 1c, we show a representative survey scan of a sample brominated for 180 min in glovebox exhibiting a strong C 1s peak (graphene) and bromine peaks of Br 3s, Br 3p, and Br 3d. The silicon peaks at 102.7 (Si 2p) and 153.6 eV (Si 2s) are related to the glass substrate carrying the FLG. The graphitic C 1s peaks for the brominated FLG samples were observed at 283.8 eV, which is downshifted from that observed for the pristine sample at 284.1 eV due to the Fermi level shift to a higher value in the negative direction (See Supporting Information, Figure S3). A high resolution scan of Br 3d peak revealed the maximum at 69.4 eV as shown in the inset of Figure 1c, which is higher than that of molecular Br_2 at (67.4 eV) and anionic Br^- (68.5 eV) and lower than covalently bonded C−Br (70.8 eV). It has been reported that bromine adsorbed on the surface of graphene should have Br 3d peak centered at 69.2 eV as compared to 70.8 eV for covalently bonded bromine.[33]

The Br 3d peak was deconvoluted into a set of three doublets using a Shirley background. The solid lines refer to the $3d_{5/2}$ peaks and dashed lines refer to $3d_{3/2}$ peaks, the doublets were constrained to an intensity ratio 3:2, respectively, with a separation of 1.05 eV.[26] According to the fitted peaks, three forms of bromine are present: (1) C_n−Br_2 charge transfer complex (67.9 eV), (2) physically adsorbed and anionic bromine (69.2 eV), and (3) covalently bonded bromine to carbon (70.0 eV).[41] Quantitative analysis of the fitted peaks reveals that after 180 min of exposure in Gbox, bromine species in FLG are generally intercalated as physically adsorbed species (1.5 at. %) and charge transfer complexes (0.9 at. %) on and between the graphene sheets, with a relatively small, but non-negligible amount of covalently bonded bromine (0.4 at. %) which is believed to be concentrated at the edges of the graphene sheets without disrupting the basal plane.

Since it is well established that bromine has an acceptor nature in graphitic materials as mentioned earlier, Br species on our brominated FLG films mostly consist of molecular Br_2 forming C_n−Br_2 complexes and anionic Br^- species that are physically adsorbed on the surface or intercalated between the graphene sheets rather than covalently bonded bromine. Hence, the increased binding energy as compared with molecular Br_2 and anionic Br^- is believed to result from the charge transfer toward Br rather than covalently bonded C−Br, which would disrupt the sp^2 planar structure of graphene. The absence of a significant peak in the C 1s spectrum at the position of covalently bonded C−Br (285.3 eV) (Figure S3a) and the negligible increase of the D-peak in the Raman spectra upon bromine exposure support the fact that the majority of bromine is physically intercalated between the graphene sheets with the possibility of a smaller number of bromine covalently bonded to carbon at defects and edge sites. The Br content (at. %) in FLG with different exposure times for samples brominated in Gbag and Gbox, are shown in Figure 1d. In both cases, the bromine content increases with increasing exposure time, which was limited to 180 min in the context of this study. However, samples treated in the Gbox exhibit higher bromine uptake indicating the influence of the exposure environment on the effectiveness of intercalation and doping processes. The higher presence of moisture in the Gbag can potentially react with anionic Br^- species on the graphene surface forming HBr in gaseous form which can further react with graphene, in addition to leaving −OH functionalities on the graphene surface and edges, which was anticipated as a potential barrier to the intercalation processes, and hence the lower uptake. The interaction of the formed HBr with FLG was further investigated by performing a control experiment of exposing FLG to vapors of HBr acid (see Supporting Information and Figure S4). It was observed that Br species resulting from HBr vapor exposure are less effective than those resulting from Br_2 exposure in enhancing the conductivity and are easily reversed by ethanol washing, indicating a minimal HBr formation in the latter case. In Figure S4b, we show the Br 3d XPS peak for Br_2−FLG and HBr−FLG in a Gbag. The stark difference in the peak positions indicates that the HBr is not present in Br_2−FLG even when prepared in a Gbag, perhaps removed after washing with ethanol.

DOI: 10.1021/acsami.5b03274
ACS Appl. Mater. Interfaces 2015, 7, 17692−17699

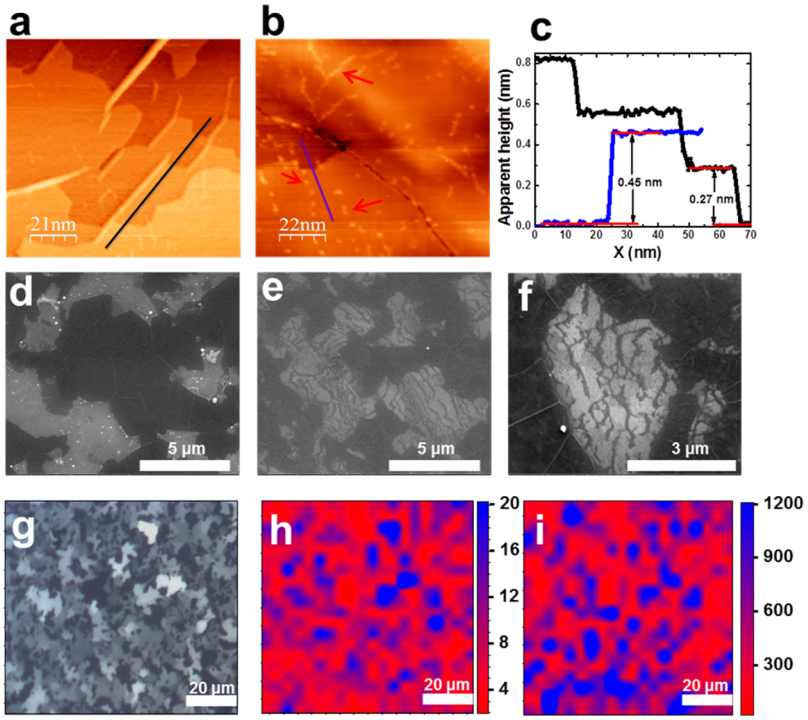

Figure 2. STM images (V_b = 0.5 V and I_t = 50 pA) of (a) pristine FLG and (b) brominated FLG (Gbag) for 180 min on nickel and (c) apparent height profiles for pristine FLG (black) and brominated FLG (blue) along the lines shown on panels a and b, respectively. SEM images of (d) pristine FLG on glass and (e, f) brominated FLG (Gbag) for 180 min on glass. (g) Optical micrograph of brominated FLG (Gbag) for 180 min and corresponding Raman maps of (h) I_G/I_D and (i) Br−Br stretching mode peak intensity.

The pristine and brominated FLG samples were studied by STM, scanning electron microscopy (SEM), atomic force microscopy (AFM), and micro-Raman imaging. The high resolution surface morphology of the pristine FLG obtained by STM is shown in Figure 2a, demonstrating a stack of 4 layers of graphene. The apparent step height between the layers was obtained by taking a line profile, indicated by the black line (Figure 2a). It shows an average interlayer spacing of 0.27 nm (Figure 2c), and is in good agreement with previous STM measurements on graphene.[42−44] STM measurements performed on the brominated FLG for 180 min (Gbag), revealed the presence of bright features (marked with red arrows in Figure 2b) forming chain-like structures throughout the surface of graphene sheets. We attribute these to adsorbed Br species, in agreement with previous studies suggesting the formation of chain channels of bromine in intercalated graphite compounds.[40,45] Furthermore, the line profile comparison of pristine and brominated FLG (Figure 2c), shows an increased average value of apparent step height by 0.18 nm which matches closely with the atomic radius of bromine, and is direct evidence of Br intercalation beneath graphene sheets. The pristine FLG transferred to a glass substrate appears to be somewhat patchy and wrinkled, as can be seen in SEM (Figure 2d) and AFM (Figure S5a) images. Upon exposure to bromine for 180 min, the multilayer regions of the FLG exhibit new surface contrast under SEM, which might be related to topographic variations (Figure 2e and f). Similar features are also seen in AFM images (Figure S5b and c) leading to the conclusion that graphene becomes locally swollen with bromine. Next, we seek to colocate changes in graphene structure with the presence of bromine. Mapping of the G-peak to D-peak intensity ratio from Raman spectra for brominated sample (Figure 2h) over the area shown by the optical image in Figure 2g indicates that a high degree of order within the FLG is preserved after bromination, especially in areas showing thicker stacks of graphene. This implies that bromine intercalates into these sheets as expected without disrupting the basal planes. Mapping of the Br−Br stretching Raman peak intensity (Figure 2i) shows that a higher intensity is correlated with the thicker, more ordered regions of FLG, consistent with a greater degree of intercalation in thicker multilayer regions, as well as with more ordered chains of Br^-. The Br−Br stretching peak is observed all over the sample, as seen in Figure 2i, which indicates that bromine is aerially present everywhere in the FLG sample.

Pristine FLG samples on glass exhibited sheet resistance ranging between 750 and 930 Ω/□ and a transmittance between 76.3 and 77.8% in the middle of the visible (550 nm). This corresponds to a FoM ranging between 1.6 and 3.3. Upon exposure to bromine, the sheet resistance drops precipitously within the first hour of exposure and gradually saturates. The sample in the GBag decreases to 45% of its starting value (Figure 3a), whereas in the GBox it decreases to 20% of its starting value, yielding a sheet resistance as low as ∼180 Ω/□. These differences are in line with XPS observations discussed earlier to the effect that the experimental environment can affect the outcome of the bromination process. In all cases, the transmittance decreased by only 2−3% of the pristine value (Figure 3b), resulting in an increase of the FoM to 3 and 7.7 for samples prepared in a GBag and a GBox, respectively. The gradual changes of sheet resistance and transmittance with increasing exposure time generally agree with the Br content as measured by XPS. We also attempted bromination by exposure to liquid bromine. Liquid bromine was drop-cast on the surface of the FLG sample on glass and allowed to evaporate at room temperature inside the Gbag. The liquid bromine was found to

DOI: 10.1021/acsami.5b03274
ACS Appl. Mater. Interfaces 2015, 7, 17692−17699

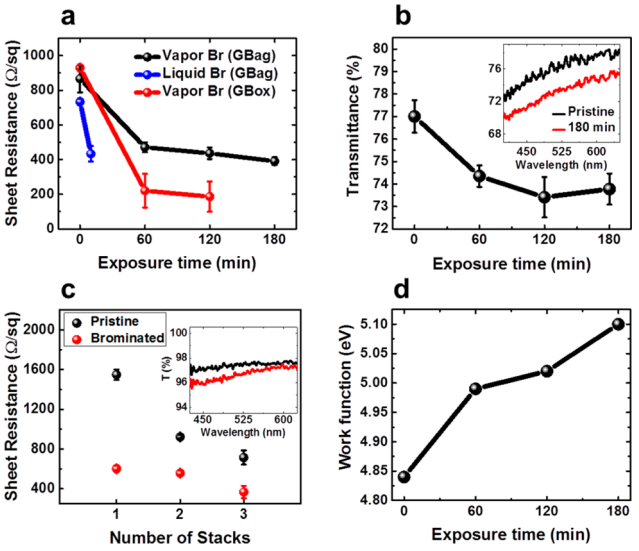

Figure 3. (a) Sheet resistance of FLG with respect to bromination time using vapor and liquid bromine sources in different inert environments. (b) Optical transmittance of vapor brominated FLG (Gbag) at 550 nm with respect to exposure time. The inset shows the transmittance spectra for pristine (black) and vapor-brominated (red) FLG after a 180 min treatment. (c) Sheet resistance of SLG, 2-LLG and 3-LLG before and after bromination for 60 min (Gbox). Inset shows the transmission spectra of SLG before and after bromination. (d) Workfunction of FLG with respect to bromine vapor exposure time (Gbag).

dry within 10 min and the sample was washed in ethanol prior to sheet resistance measurement. We find the sheet resistance reaches the same level after 10 min of liquid bromination as was achieved after 180 min of vapor bromination, indicating the latter method can also be effective at doping graphene. We have also evaluated the vapor phase bromination of SLG and LLG samples (Figure 3c). In case of SLG, the sheet resistance drops from 1548 Ω/□ for the pristine sample to 602 Ω/□ after exposure to bromine for 60 min. The transmittance decreased very slightly by 0.8% (inset of Figure 3c), resulting in a FoM increase from 9.5 to 15.6. The sheet resistance decreases more modestly for two and three LLG samples. We have performed Hall effect measurements on brominated FLG samples (Gbag) and show that FLG becomes p-doped by bromination. Enhancement of the conductivity is shown to result from the doubling of the carrier concentration upon bromination (from 2.9×10^{13} to 5.7×10^{13} cm^{-2}), due to charge transfer from FLG to bromine molecules. Bromination of FLG also modified the work function, increasing it from 4.84 to 5.10 eV after bromine vapor exposure for 180 min (Figure 3d). The upshift in the work function is believed to result from the shift in the Fermi energy level toward the valence band of FLG upon charge transfer to bromine.

The stability in ambient air of brominated SLG and FLG was evaluated by measuring sheet resistance after leaving samples in ambient air for 10 days. In these conditions, bromine is expected to desorb with time toward its residue compound in a similar manner as intercalated graphite compounds.[29] FLG samples are found to remain stable in air, while the sheet resistance of SLG sample increases by 50% (Figure 4a). This indicates that intercalated bromine in the FLG sample is protected from desorption and reactivity, comparing very favorably to the aging in air of $AuCl_3$-doped graphene,[46] which degrades over time. As expected, SLG samples are probably more prone to loss of Br. We have further investigated the stability of brominated FLG samples by placing them on a hot plate for 10 min at fixed temperature in a nitrogen glovebox and measuring their sheet resistance (Figure 4b). We find the sheet resistance increases slowly and monotonically up to 150 °C toward the pristine FLG sheet resistance along with a decrease in the Br atomic content due to desorption. Beyond this temperature, the sheet resistance increases above the pristine value, hinting that graphene and bromine may potentially undergo a chemical reaction or structural changes resulting from a phase change at elevated temperature (for more details, including XPS analysis, see Supporting Information).

Our results have thus far indicated that bromine doping of graphene electrodes can result in a large enhancement of conductivity with minor cost in optical transmittance, but without quantitatively comparing them to other doping schemes reported previously. We have plotted in Figure 5a the ratio of the decrease of sheet resistance with respect to the change in transmittance ($\Delta R_S/\Delta T$) of brominated graphene samples and compared it with various other treatments reported in the literature, including metal chlorides, acid doping and other approaches.[18,19,22,46,47] The raw data of sheet resistance and transmittance before and after treatment are shown in the inset of Figure 5a, with a line linking the data points to highlight the differences in the steepness of the slope. We find that bromine doping of graphene outperforms almost

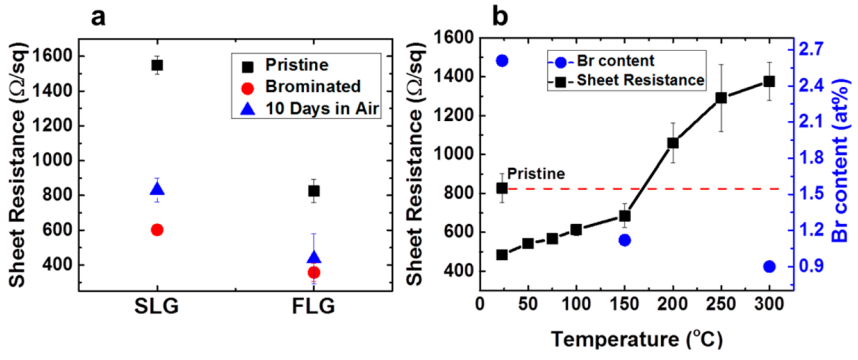

Figure 4. Stability of brominated graphene (Gbox). (a) Sheet resistance of brominated SLG and FLG after leaving for 10 days in air at room temperature and (b) stability of sheet resistance of FLG graphene after thermal annealing in a Gbox for 10 min heating intervals at each temperature and corresponding bromine content at selected times as deduced from XPS measurements. The samples were allowed to cool down to room temperature before measuring the sheet resistance.

DOI: 10.1021/acsami.5b03274
ACS Appl. Mater. Interfaces 2015, 7, 17692−17699

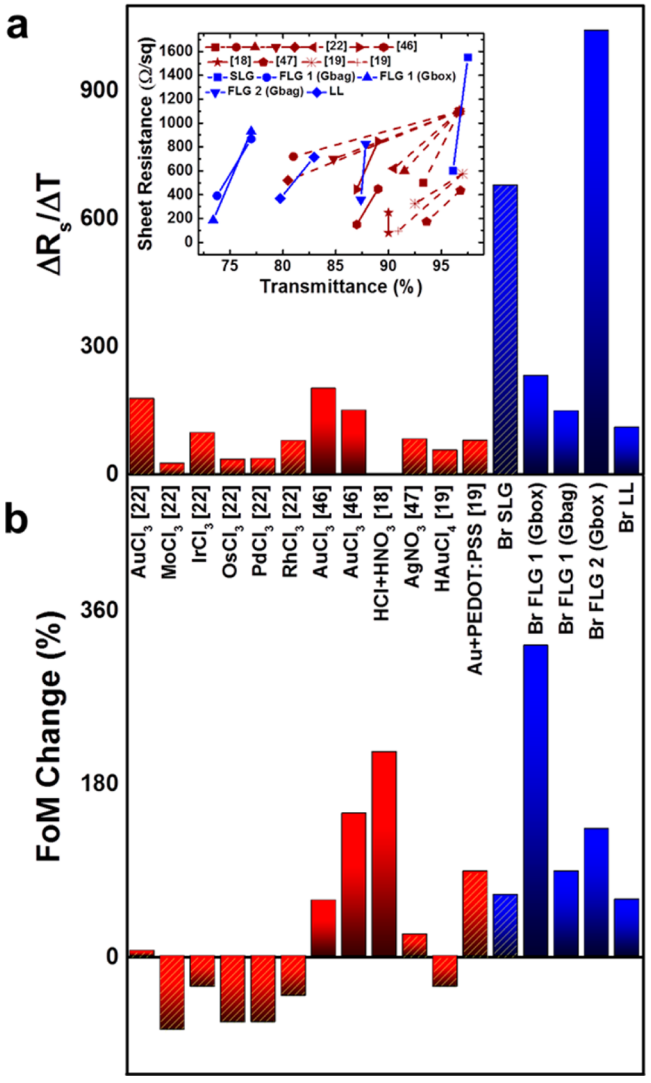

Figure 5. (a) Decrease in sheet resistance with respect to the change of transmittance for several doping methods reported in the literature (red) and in this work (blue). The inset shows the raw sheet resistance and transmittance data. (b) Percentage change of the figure of merit (FoM) for different doping methods reported in the literature (red) and in this work (blue). Hash patterns in panels a and b correspond to SLG with all the rest referring to FLG samples. $\Delta R_S/\Delta T$ is not shown for acid doping (ref 18) because ΔT was reported to be zero.

all results in the literature in terms of $\Delta R_S/\Delta T$ for both SLG (shaded bars) and FLG (solid bars), with the exception of acid-doped graphene.[18] In Figure 5b, we have plotted the percentage change of FoM for a wide range of results in the literature which provide sheet resistance and transmission change data and compared it to bromine doping of SLG and FLG graphene. The results indicate that we have achieved the highest enhancement of FoM when compared to other doping schemes for FLG. The performance enhancement of FLG was greater than that of SLG. We attribute this to the ability of bromine to decorate the surface, grain boundaries, step edges and intercalate between the layers of FLG, whereas in SLG it is mainly adsorbed on the surface and at grain boundaries.

In summary, we have successfully demonstrated p-doping of graphene with bromine, resulting in a significant reduction of sheet resistance at minimal cost to optical transmission. The air stability of the bromination approach for FLG in ambient conditions indicates this method may be technologically applicable. Comparison and benchmarking of the performance of Br-doped graphene in terms of $\Delta R_S/\Delta T$ and FoM with previously reported doping schemes reveals that bromination is significantly more effective than most previously reported methods, making this approach potentially suitable for a wide range of optoelectronic applications requiring highly transparent conducting electrodes.

EXPERIMENTAL METHODS

Sample Preparation and Doping. Single-layer graphene (SLG) was synthesized by a modified low pressure chemical vapor deposition (CVD) process, where the copper foil is sandwiched between two quartz substrates to reduce evaporation from the foil during the annealing and growth process (for more information see Supporting Information).[48] Commercially available few layers graphene (FLG) CVD grown on 300 nm nickel films on SiO_2/Si substrate were also used. Graphene samples were transferred to glass substrate using the conventional PMMA transfer method[36] followed by annealing for 90 min at 450 °C in argon and hydrogen atmosphere.

Graphene samples transferred to glass were exposed to bromine vapor or liquid at room temperature either inside a glovebag filled with nitrogen and placed in a fume hood (2000 ppm of O_2 and 2500 ppm for H_2O) or a nitrogen glovebox with less than 0.1 ppm of oxygen and moisture. For vapor exposure of FLG samples to bromine, the sample was suspended in a sealed container holding liquid bromine kept at room temperature. The bromine is expected to reach its room temperature equilibrium vapor pressure of 270 mbar inside the sealed container.[49] The bromine uptake was controlled simply by the exposure time inside the sealed container. The samples were washed with ethanol to remove weakly bound bromine molecules.

Characterization. X-ray photoelectron spectroscopy was performed using an Omicron Nanotechnology (Taunusstein, Germany) UHV system with a monochromatic Al source (1486.7 eV). A hemispherical energy analyzer EIS-Sphera was used to measure the XPS spectra. Core-level XPS scans of carbon 1s and bromine 3p and 3d regions were acquired at a pass energy of 20 eV and a step size of 0.05 eV. A base pressure of about 4.0×10^{-10} mbar was maintained throughout all measurements. The spectroscopic data were processed using CasaXPS software (Casa Software Ltd.).

Scanning tunneling microscopy (STM) imaging was performed in ultrahigh vacuum conditions (5.0×10^{-10} mbar) in a variable temperature STM (VT-STM; Omicron Nanotechnology). Graphene samples were kept at room temperature during measurements. A chemically etched polycrystalline tungsten STM tip was used for imaging, which was further cleaned by electron bombardment in situ in UHV to reach atomically resolved imaging of HOPG. FLG samples on sputtered Ni on SiO_2/Si were mounted on a sample plate for STM studies. All images were acquired with a sample bias of $V_b = 0.5$ V and a tunneling current of $I_t = 50$ pA.

Raman spectra and maps were obtained using a LabRAM ARAMIS (Horiba Jobin Yvon, Inc.) instrument. The excitation source was a 473 nm laser, focused with a 100× objective with a laser spot of 1 μm and 0.5 mW power. The scattered signal was dispersed with a 1800 mm^{-1} grating. The spectra ranging from 1200 to 2900 cm^{-1} were collected in backscattering geometry.

A 4-point probe was used to measure the sheet resistance of the samples. Optical transmittance measurements were performed using a F20-UVX spectrometer (Filmetrics, Inc.) equipped with tungsten halogen and deuterium light sources over the range from 400 to 700 nm. Work function measurements were performed using photoelectron spectroscopy in Air (PESA) system (RKI, Inc.) with UV excitation energy of 100 nW.

ASSOCIATED CONTENT

Supporting Information

The Supporting Information is available free of charge on the ACS Publications website at DOI: 10.1021/acsami.5b03274.

DOI: 10.1021/acsami.5b03274
ACS Appl. Mater. Interfaces 2015, 7, 17692−17699

Additional information on the modified configuration for CVD of SLG, Raman analysis of the G-peak, high-resolution XPS spectra of C1 s and Br 3p, stability of doped graphene, comparison of bromine doping of graphene via Br_2 and HBr vapor exposures, AFM images, and the calculation methods of the FoM changes (PDF)

AUTHOR INFORMATION

Corresponding Author

*E-mail: aram.amassian@kaust.edu.sa.

Author Contributions

The manuscript was written through contributions of all authors. All authors have given approval to the final version of the manuscript.

Notes

The authors declare no competing financial interest.

ACKNOWLEDGMENTS

The authors acknowledge Dr. Habib Katsiev of SABIC Corporate Research and Innovation Center, Saudi Arabia for discussion of STM results, Dr. Cecilia Mattevi and Prof. Norbert Klein of the department of materials, Imperial College, for their help and training on graphene CVD on copper foil and transfer, as well as Dr. Issam Gereige of the Solar and Photovoltaic Engineering Research Center, KAUST for his assistance with Hall effect measurements.

REFERENCES

(1) Novoselov, K. S.; Geim, A. K.; Morozov, S. V.; Jiang, D.; Zhang, Y.; Dubonos, S. V.; Grigorieva, I. V.; Firsov, A. A. Electric Field Effect in Atomically Thin Carbon Films. *Science* **2004**, *306*, 666−669.

(2) Lu, W.; Soukiassian, P.; Boeckl, J. Graphene: Fundamentals and Functionalities. *MRS Bull.* **2012**, *37*, 1119−1124.

(3) Lee, C.; Wei, X.; Kysar, J. W.; Hone, J. Measurement of the Elastic Properties and Intrinsic Strength of Monolayer Graphene. *Science* **2008**, *321*, 385−388.

(4) Nan, H. Y.; Ni, Z. H.; Wang, J.; Zafar, Z.; Shi, Z. X.; Wang, Y. Y. The Thermal Stability of Graphene in Air Investigated by Raman Spectroscopy. *J. Raman Spectrosc.* **2013**, *44*, 1018−1021.

(5) Balandin, A. A.; Ghosh, S.; Bao, W.; Calizo, I.; Teweldebrhan, D.; Miao, F.; Lau, C. N. Superior Thermal Conductivity of Single-Layer Graphene. *Nano Lett.* **2008**, *8*, 902−907.

(6) Morozov, S. V.; Novoselov, K. S.; Katsnelson, M. I.; Schedin, F.; Elias, D. C.; Jaszczak, J. A.; Geim, A. K. Giant Intrinsic Carrier Mobilities in Graphene and Its Bilayer. *Phys. Rev. Lett.* **2008**, *100*, 016602.

(7) Nair, R. R.; Blake, P.; Grigorenko, A. N.; Novoselov, K. S.; Booth, T. J.; Stauber, T.; Peres, N. M. R.; Geim, A. K. Fine Structure Constant Defines Visual Transparency of Graphene. *Science* **2008**, *320*, 1308−1308.

(8) Bonaccorso, F.; Sun, Z.; Hasan, T.; Ferrari, A. C. Graphene Photonics and Optoelectronics. *Nat. Photonics* **2010**, *4*, 611−622.

(9) Bae, S.; Kim, H.; Lee, Y.; Xu, X.; Park, J.-S.; Zheng, Y.; Balakrishnan, J.; Lei, T.; Kim, H. R.; Song, Y. I.; Kim, Y.-J.; Kim, K. S.; Özyilmaz, B.; Ahn, J.-H. Roll-to-Roll Production of 30-Inch Graphene Films for Transparent Electrodes. *Nat. Nanotechnol.* **2010**, *5*, 574−578.

(10) Park, H.; Chang, S.; Zhou, X.; Kong, J.; Palacios, T.; Gradečak, S. Flexible Graphene Electrode-Based Organic Photovoltaics with Record-High Efficiency. *Nano Lett.* **2014**, *14*, 5148−5154.

(11) Park, H.; Chang, S.; Smith, M.; Gradečak, S.; Kong, J. Interface Engineering of Graphene for Universal Applications as Both Anode and Cathode in Organic Photovoltaics. *Sci. Rep.* **2013**, *3*, 1581.

(12) Hurd, A. J.; Kelley, R. L.; Eggert, R. G.; Lee, M.-H. Energy-Critical Elements for Sustainable Development. *MRS Bull.* **2012**, *37*, 405−410.

(13) de Jong, M. P.; van Ijzendoorn, L. J.; de Voigt, M. J. A. Stability of the Interface between Indium-Tin-Oxide in Polymer Light-Emitting Diodes. *Appl. Phys. Lett.* **2000**, *77*, 2255−2257.

(14) Ellmer, K. Past Achievements and Future Challenges in the Development of Optically Transparent Electrodes. *Nat. Photonics* **2012**, *6*, 809−817.

(15) Du, J.; Pei, S.; Ma, L.; Cheng, H. 25th Anniversary Article: Carbon Nanotube- and Graphene-Based Transparent Conductive Films for Optoelectronic Devices. *Adv. Mater.* **2014**, *26*, 1958−1991.

(16) De, S.; Higgins, T. M.; Lyons, P. E.; Doherty, E. M.; Nirmalraj, P. N.; Blau, W. J.; Boland, J. J.; Coleman, J. N. Silver Nanowire Networks as Flexible, Transparent, Conducting Films: Extremely High DC to Optical Conductivity Ratios. *ACS Nano* **2009**, *3*, 1767−1774.

(17) Mattevi, C.; Kim, H.; Chhowalla, M. A Review of Chemical Vapour Deposition of Graphene on Copper. *J. Mater. Chem.* **2011**, *21*, 3324−3334.

(18) Wang, Y.; Tong, S. W.; Xu, X. F.; Ozyilmaz, B.; Loh, K. P. Interface Engineering of Layer-by-Layer Stacked Graphene Anodes for High-Performance Organic Solar Cells. *Adv. Mater.* **2011**, *23*, 1514−1518.

(19) Liu, Z.; Li, J.; Sun, Z.-H.; Tai, G.; Lau, S.-P.; Yan, F. The Application of Highly Doped Single-Layer Graphene as the Top Electrodes of Semitransparent Organic Solar Cells. *ACS Nano* **2012**, *6*, 810−818.

(20) Kim, Y.; Ryu, J.; Park, M.; Kim, E. S.; Yoo, J. M.; Park, J.; Kang, J. H.; Hong, B. H. Vapor-Phase Molecular Doping of Graphene for High-Performance Transparent Electrodes. *ACS Nano* **2014**, *8*, 868−874.

(21) Kwon, K. C.; Choi, K. S.; Kim, C.; Kim, S. Y. Effect of Transition-Metal Chlorides on Graphene Properties. *Phys. Status Solidi A* **2014**, *211*, 1794−1800.

(22) Kwon, K. C.; Choi, K. S.; Kim, S. Y. Increased Work Function in Few-Layer Graphene Sheets via Metal Chloride Doping. *Adv. Funct. Mater.* **2012**, *22*, 4724−4731.

(23) Hennig, G. The Properties of the Interstitial Compounds of Graphite. III. The Electrical Properties of the Halogen Compounds of Graphite. *J. Chem. Phys.* **1952**, *20*, 1443−1447.

(24) Sasa, T.; Takahashi, Y.; Mukaibo, T. Electrical Conductivity of Graphite Bromine Lamellar Compounds. *Bull. Chem. Soc. Jpn.* **1970**, *43*, 34−38.

(25) Lee, R. S.; Kim, H. J.; Fischer, J. E.; Thess, A. Conductivity Enhancement in Single-Walled Carbon Nanotube Bundles Doped with K and Br. *Nature* **1997**, *388*, 255−257.

(26) Bulusheva, L. G.; Okotrub, A. V.; Flahaut, E.; Asanov, I. P.; Gevko, P. N.; Koroteev, V. O.; Fedoseeva, Y. V.; Yaya, A.; Ewels, C. P. Bromination of Double-Walled Carbon Nanotubes. *Chem. Mater.* **2012**, *24*, 2708−2715.

(27) Ikemoto, I.; Cao, Y.; Yamada, M.; Kuroda, H.; Harada, I.; Shirakawa, H.; Ikeda, S. X-Ray Photoelectron Spectroscopic Study of Highly Conductive Bromine-Doped Polyacetylene. *Bull. Chem. Soc. Jpn.* **1982**, *55*, 721−725.

(28) Tongay, S.; Hwang, J.; Tanner, D. B.; Pal, H. K.; Maslov, D.; Hebard, A. F. Supermetallic Conductivity in Bromine-Intercalated Graphite. *Phys. Rev. B: Condens. Matter Mater. Phys.* **2010**, *81*, 115428.

(29) Dresselhaus, M. S.; Dresselhaus, G. Intercalation Compounds of Graphite. *Adv. Phys.* **2002**, *51*, 1−186.

(30) Jung, N.; Kim, N.; Jockusch, S.; Turro, N. J.; Kim, P.; Brus, L. Charge Transfer Chemical Doping of Few Layer Graphenes: Charge Distribution and Band Gap Formation. *Nano Lett.* **2009**, *9*, 4133−4137.

(31) Fan, X.; Liu, L.; Kuo, J.-L.; Shen, Z. Functionalizing Single- and Multi-Layer Graphene with Br and Br_2. *J. Phys. Chem. C* **2010**, *114*, 14939−14945.

(32) Ueno, K.; Kosugi, R.; Imazeki, K.; Aozasa, A.; Matsumoto, Y.; Miyazaki, H.; Sakuma, N.; Kajita, A.; Sakai, T. Bromine Doping of Multilayer Graphene for Low-Resistance Interconnects. *Jpn. J. Appl. Phys.* **2014**, *53*, 05GC02.

DOI: 10.1021/acsami.5b03274
ACS Appl. Mater. Interfaces 2015, 7, 17692−17699

(33) Zheng, J.; Liu, H.-T.; Wu, B.; Di, C.-A.; Guo, Y.-L.; Wu, T.; Yu, G.; Liu, Y.-Q.; Zhu, D.-B. Production of Graphite Chloride and Bromide Using Microwave Sparks. *Sci. Rep.* **2012**, *2*, 662.
(34) Song, J. J.; Chung, D. D. L.; Eklund, P. C.; Dresselhaus, M. S. Raman Scattering in Graphite Intercalation Compounds. *Solid State Commun.* **1976**, *20*, 1111−1115.
(35) Li, J.; Vaisman, L.; Marom, G.; Kim, J. K. Br Treated Graphite Nanoplatelets for Improved Electrical Conductivity of Polymer Composites. *Carbon* **2007**, *45*, 744−750.
(36) Li, X.; Zhu, Y.; Cai, W.; Borysiak, M.; Han, B.; Chen, D.; Piner, R. D.; Colombo, L.; Ruoff, R. S. Transfer of Large-Area Graphene Films for High-Performance Transparent Conductive Electrodes. *Nano Lett.* **2009**, *9*, 4359−4363.
(37) Casiraghi, C.; Hartschuh, a; Qian, H.; Piscanec, S.; Georgi, C.; Fasoli, a; Novoselov, K. S.; Basko, D. M.; Ferrari, a C. Raman Spectroscopy of Graphene Edges. *Nano Lett.* **2009**, *9*, 1433−1441.
(38) Kim, K. S.; Zhao, Y.; Jang, H.; Lee, S. Y.; Kim, J. M.; Kim, K. S.; Ahn, J.-H.; Kim, P.; Choi, J.-Y.; Hong, B. H. Large-Scale Pattern Growth of Graphene Films for Stretchable Transparent Electrodes. *Nature* **2009**, *457*, 706−710.
(39) Das, A.; Pisana, S.; Chakraborty, B.; Piscanec, S.; Saha, S. K.; Waghmare, U. V.; Novoselov, K. S.; Krishnamurthy, H. R.; Geim, A. K.; Ferrari, A. C.; Sood, A. K. Monitoring Dopants by Raman Scattering in an Electrochemically Top-Gated Graphene Transistor. *Nat. Nanotechnol.* **2008**, *3*, 210−215.
(40) Eklund, P.; Kambe, N.; Dresselhaus, G.; Dresselhaus, M. In-Plane Intercalate Lattice Modes in Graphite-Bromine Using Raman Spectroscopy. *Phys. Rev. B: Condens. Matter Mater. Phys.* **1978**, *18*, 7069−7079.
(41) Papirer, E.; Lacroix, R.; Donnet, J.; Nanse, G.; Fioux, P. XPS STUDY OF THE HALOGENATION OF CARBON BLACK - PART 1. BROMINATION. *Carbon* **1994**, *32*, 1341−1358.
(42) Feng, X.; Salmeron, M. Electronic Screening in Stacked Graphene Flakes Revealed by Scanning Tunneling Microscopy. *Appl. Phys. Lett.* **2013**, *102*, 053116.
(43) Poon, S. W.; Chen, W.; Wee, A. T. S.; Tok, E. S. Growth Dynamics and Kinetics of Monolayer and Multilayer Graphene on a 6H-SiC(0001) Substrate. *Phys. Chem. Chem. Phys.* **2010**, *12*, 13522−13533.
(44) Wang, Q.; Zhang, W.; Wang, L.; He, K.; Ma, X.; Xue, Q. Large-Scale Uniform Bilayer Graphene Prepared by Vacuum Graphitization of 6H-SiC(0001) Substrates. *J. Phys.: Condens. Matter* **2013**, *25*, 095002.
(45) Eeles, W. T.; Turnbull, J. A. The Crystal Structure of Graphite-Bromine Compounds. *Proc. R. Soc. London, Ser. A* **1965**, *283*, 179−193.
(46) Kim, K. K.; Reina, A.; Shi, Y.; Park, H.; Li, L.-J.; Lee, Y. H.; Kong, J. Enhancing the Conductivity of Transparent Graphene Films via Doping. *Nanotechnology* **2010**, *21*, 285205.
(47) Shin, D. H.; Lee, K. W.; Lee, J. S.; Kim, J. H.; Kim, S.; Choi, S.-H. Enhancement of the Effectiveness of Graphene as a Transparent Conductive Electrode by $AgNO_3$ Doping. *Nanotechnology* **2014**, *25*, 125701.
(48) Chen, S.; Ji, H.; Chou, H.; Li, Q.; Li, H.; Suk, J. W.; Piner, R.; Liao, L.; Cai, W.; Ruoff, R. S. Millimeter-Size Single-Crystal Graphene by Suppressing Evaporative Loss of Cu during Low Pressure Chemical Vapor Deposition. *Adv. Mater.* **2013**, *25*, 2062−2065.
(49) Fischer, J.; Bingle, J. The Vapor Pressure of Bromine from 24 to 116°. *J. Am. Chem. Soc.* **1955**, *77*, 6511−6512.

DOI: 10.1021/acsami.5b03274
ACS Appl. Mater. Interfaces 2015, 7, 17692−17699